Scaling factor for the A-ref1 configuration of the SWGO array

I.D. Vergara Quispe[1], P.M. Hansen[1], L. Nellen[2], A.G. Mariazzi[1] and D.G. Melo[3]

[1] *Instituto de Física La Plata, La Plata, Argentina.*

[2] *Instituto de Ciencias Nucleares, UNAM,Coyoacán, México.*

[3] *ITeDA, Buenos Aires, Argentina.*

22nd May 2024

Several air shower observables exhibit sensitivity to the geometric layout of the detector array. In this note, we present an analysis of the A-ref1 configuration within the SWGO (The Southern Wide-field Gamma-ray Observatory) array.
The results yield a crucial scaling factor that establishes a linkage for these observables between the central and outrigger arrays.
Examining the A-ref1 configuration helps reveal how array geometry impacts observable outcomes. The conclusions highlight the importance of understanding and considering these geometric effects when interpreting air shower data.

1 Introduction

The SWGO array consists of detectors that exhibit diverse densities across its configuration. This feature highlights the crucial need for a thorough investigation to identify the best approach for incorporating this density-related effect.

Understanding how to effectively account for these varying densities within the array is essential for accurate data interpretation and reliable observation outcomes.

It is advisable to study this effect specially for air shower observables that are sensitive to these array density variations like S_b , station multiplicity, etc.

This investigation was undertaken within the framework of SWGO's A-ref1 configuration, which is described in section 2. In section 3 it is explained how the scaling factor linking the central and outrigger array was found. The implementation of the scaling factor in some example shower observables is described in section 4 and the conclusions are in section 5.

2 Geometry of A-ref1 configuration

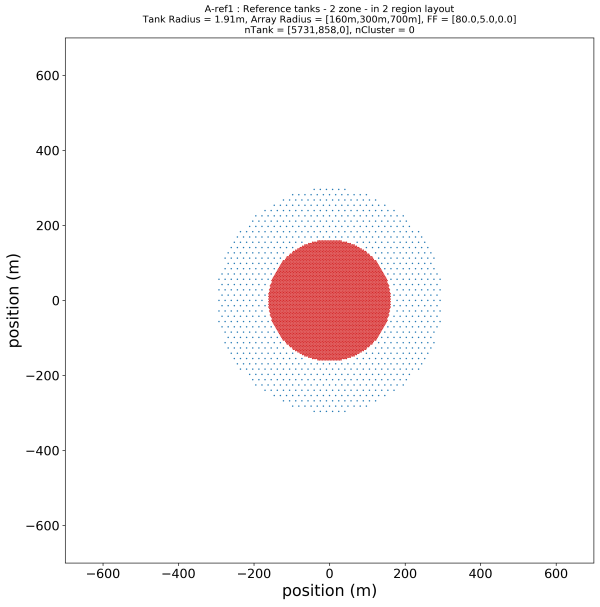

Fig. 1 Schema of the SWGO detector design: central array in red, outrigger array in blue. [1]

At this stage of SWGO, different candidate designs for the array have been proposed. Among them, the A-ref1 configuration currently serves as the reference array. This design employs water Cherenkov detector

stations with a tank radius of 1.91 m. It includes a denser core area extending up to a radius of 160 m, incorporating a total of 5731 stations (fill factor: FF = 80%). This is followed by a lower density outer array, or outrigger area, extending to a radius of 300 m and containing a total of 858 stations (fill factor: FF = 5%), as shown in Figure 1. The separation between stations is set at approximately 0.25 m for the central array and 12.45 m for the outrigger array.

Each station will have two PMTs —one positioned to observe the top compartment and the another the bottom compartment— both aligned with the station's cylindrical axis. The stations form a triangular grid with a spacing of 4.07 m for the central array and 16.27 m for the outrigger.

3 Relation between central and outrigger array

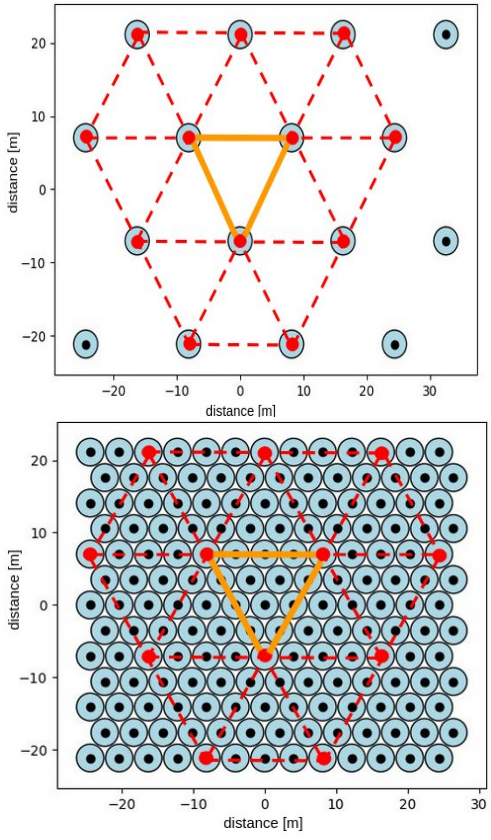

Fig. 2 The red lines demarcate the boundaries of the unit cells, while the yellow lines indicate the unit cell under observation for different configurations of the SWGO array. On the top side is the outrigger configuration, while on the bottom side is the central array configuration.

Many air shower observables are designed for uniform array setups. However, in the context of SWGO, the array displays varying densities, leading to deviations in the calculation of these observables. To tackle this issue, a scaling factor is applied to alleviate these discrepancies.

A preliminary method for calculating the scaling factor involves utilizing the ratio of detector densities between the central and outrigger arrays. To mitigate edge effects resulting from non-uniform station distributions, this analysis considers stations within a distance of 150 m from the array center (A_{150} = 70686 m^2, and 4939 stations), corresponding to the central array, as well as stations within a radius greater than 170 m ($A_{170-300}$ = 191951 m^2, and 840 stations), corresponding to the outrigger array. The ratio of the area occupied by stations to the total number of stations in each configuration (228.51 m^2/station for outrigger, and 14.31 m^2/station for central array) is found to be 16, serving as the scaling factor.

Another approach for calculating the scaling factor involved constructing a unit cell using the three closest stations from the outrigger array. Figure 2 (top) illustrates the unit cell under investigation, highlighted by the yellow-colored sides, along with neighboring unit cells formed by stations surrounding it in the outrigger array.

Each station in the unit cell shares a common vertex with six neighboring cells. Thus, the analysis shows that the three stations in the unit cell collectively contribute only half a station per cell.

By applying the same procedure to the central array with a unit cell size similar to the outrigger array (see Figure 2), one must consider common side stations, inside unit cell stations, and stations with common vertices:

- The contribution from the common vertices remains the same as in the outrigger array, accounting for half a station per cell.
- Three common side stations are shared by two unit cells, resulting in a contribution of 3/2 stations per side per unit cell. Each cell has 3 sides contributing 9/2 stations per cell.
- Additionally, each cell has 3 internal stations, not shared with other cells, contributing 3 stations per cell.

Therefore, the total contribution of stations per unit cell in the central array is equal to 1/2 + 9/2 + 3 = 8. By comparing the central array's contribution of 8 stations to the outrigger array's 0.5 stations, it becomes evident

that there are 16 stations in the central array for every station present in the outrigger array. This comparison confirms the scaling factor to be 16.

The central array can adopt the outrigger configuration by removing the inner stations from the central array and retaining only those corresponding to the outrigger station density, see figure 3.

In Figure 3, it can be seen a portion of the central array adopting the outrigger configuration masking most of the original configuration station with no symbol. However, SWGO array could not be considered as an uniformed array by extending the outrigger configuration to the central array due to this uniformity is broken in the edges.

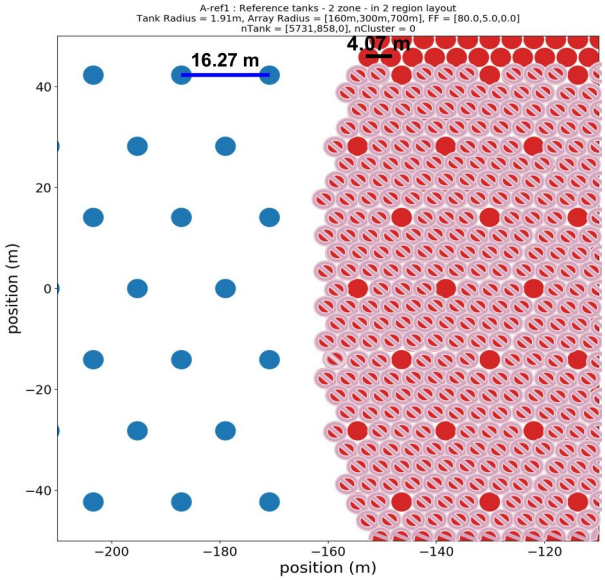

Fig. 3 Schema of the part of the central array in red adopting the outrigger configuration.

4 Implementation examples of the scaling factor

In this section, an implementation of the scaling factor in two observables, S_b and the total number of trigger stations, is presented.

4.1 S_b

The observable S_b [2] has been utilized in the Pierre Auger Observatory (PAO) for the purpose of gamma hadron separation. It is defined as follows [2]:

$$S_b = \sum_{i=1}^{N} \left[S_i \times \left(\frac{r_i}{r_0} \right)^b \right] \quad (1)$$

where the sum runs over all the triggered stations, S_i is the signal recorded in the ith station, r_i is the distance of this station to the shower axis, r_0 is a distance of reference, and the parameter b is a free parameter, allowing for the maximization of the discriminating power of this observable. For SWGO, the signal from the PMT positioned at the top of the tank is used to calculate S_b.

The scaling factor's implementation in the S_b observable is validated by mimicking the outrigger configuration in the central array. This is done by including in the calculation only the stations that match the outrigger station density.

The observable S_b is then calculated for both central array configurations [2]:

- First, for the original configuration (see Figure 1). This configuration represents the denser array, utilizing the standard calculation of $S_b = \sum_{i=1}^{N} \left[S_i \times \left(\frac{r_i}{100} \right)^b \right]$ considering all the PMTs that trigger the central array.
- Next, for the modified configuration (see Figure 3). In this configuration, the central array has been adjusted to resemble the outrigger array by excluding certain stations. The calculation of S_b incorporates the scaling factor: $S_b = \sum_{i=1}^{N} \left[S_i \times \left(\frac{r_i}{100} \right)^b \times 16 \right]$ to account for the dismissed stations and the change in the array configuration.

The same events were used in both configurations for comparing the results.

By calculating S_b for these two configurations, a comparison can be made to determine the effect of the scaling factor. This analysis helps in verifying whether the scaling factor accurately represents the relationship between the central and outrigger arrays.

In order to ensure that a significant portion of the shower is well contained within the array and to avoid potential irregularities at the array boundaries, the analysis focused on events with a core distance smaller than 50 meters from the center of the array. In Figure 4, the relative difference of the results for S_b obtained using the two methods described above is presented.

The distribution has a deviation smaller than 20% centered at zero, demonstrating that both sets of results closely match each other, indicating that the scaling factor of 16 successfully reproduces the results

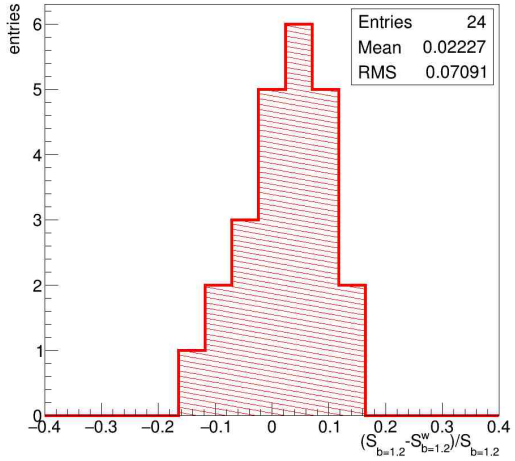

Fig. 4 Relative difference of S_b values obtained through standard and weighted calculations.

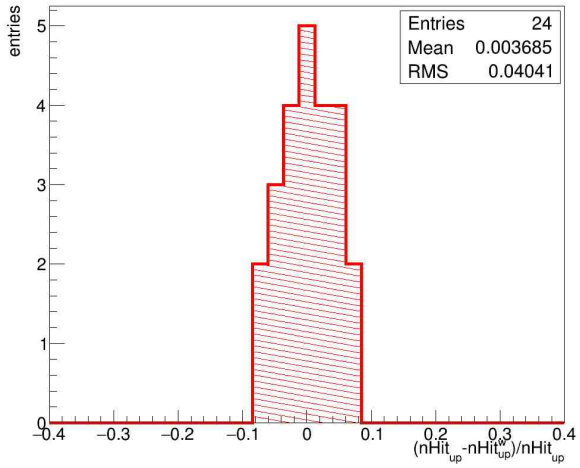

Fig. 5 Relative difference of the station multiplicity ($nHit_{up}$) values obtained through standard and weighted calculations.

obtained in the central array when using the outrigger configuration.

4.2 Total number of triggered stations

The total number of triggered stations in an event is a crucial parameter that reflects the size of the shower.

Due to the distinct densities present in the SWGO array, it is recommended to adjust the total number of triggered stations in an event using a scaling factor that accounts for these variations in density.

The total number of triggered stations, $nHit_{up}$, is computed using the PMT at the top of the tank. When a station is in the outrigger array, its $nHit_{up}$ count is multiplied by 16 before being included in the calculation.

To assess the validity of this procedure, we calculate $nHit_{up}$ using the two configurations that were employed in the preceding section. Figure 5 displays the relative difference between the total number of hits in the top PMT ($nHit_{up}$) and the corresponding scaled value ($nHit^{w}_{up}$).

In this instance, the distribution exhibits a deviation of less than 10% centered around zero. This illustrates a close alignment between both sets of results, confirming that the scaling factor of 16 effectively replicates the outcomes obtained from the central array when utilizing the outrigger configuration.

It should be emphasized the importance of using the scaling factor when computing $nHit_{up}$, especially for selecting showers of the same size covering both the central array and the outriggers.

5 Conclusion

In conclusion, when working with arrays of varying densities, implementing a scaling factor is essential to avoid bias in the calculations. This is particularly crucial for observables dependent on array density, such as S_b and $nHit_{up}$.

This note focused on studying the A-ref1 configuration as an example to elucidate the influence of array geometry on observable results. It underscores the critical importance of incorporating these geometric effects when interpreting data from air showers.

Future work may include the study of edge effects, applications to other reconstructed shower observables of SWGO, and exploring these geometric effects for other candidate designs proposed for the SWGO array.

Acknowldegements LN would like to acknowledge support by DGPA-PAPIIT IN110621.

References

[1] R. Conceição et al. *Detector unit and array configurations for M5*. Tech. rep. SWGO-A&S-21-001. SWGO, 2022. URL: https://www.swgo.org/SWGOWiki/lib/exe/fetch.php?media=simulations:swgo_m5_configurations-v3.pdf.

[2] G. Ros et al. 'Improving photon-hadron discrimination based on cosmic ray surface detector data'. In: *Astroparticle Physics* 47 (2013), pp. 10–17. DOI: 10.1016/j.astropartphys.2013.05.014.